Journal of Alloys and Compounds 523 (2012) 102–107

Contents lists available at SciVerse ScienceDirect

Journal of Alloys and Compounds

journal homepage: www.elsevier.com/locate/jallcom

New solid solution $Fe_{1-x}Cr_xVSbO_6$ with rutile-type structure

E. Filipek*, G. Dąbrowska

West Pomeranian University of Technology, Szczecin, Faculty of Chemical Technology and Engineering, al. Piastów 42, 71–065 Szczecin, Poland

ARTICLE INFO

Article history:
Received 9 October 2011
Received in revised form 10 January 2012
Accepted 16 January 2012
Available online 2 February 2012

Keywords:
$Fe_{1-x}Cr_xSbVO_6$ solid solution
IR
SEM
XRD

ABSTRACT

A new solid solution with formula $Fe_{1-x}Cr_xVSbO_6$ has been prepared by the conventional solid-state reaction technique using the starting mixtures containing V_2O_5, α-Sb_2O_4, Cr_2O_3 and Fe_2O_3 as well as $FeVSbO_6$ and $CrVSbO_6$. Continuous substitutional solid solution of a tetragonal structure of rutile-type in the $FeVSbO_6$–$CrVSbO_6$ system is formed in the whole concentration range $0.0 < x < 1.0$. The solid solution was characterised by XRD, DTA-TG, IR and SEM/EDX methods. With increasing degree of Cr^{3+} ion incorporation into the $FeVSbO_6$ structure, the contraction of $Fe_{1-x}Cr_xVSbO_6$ solid solution crystal lattice increased. The temperature of its thermal stability in the solid state was established and gradual shifting of the corresponding IR absorption bands towards higher wave numbers was observed.

1. Introduction

From amongst many oxides, the following ones V_2O_5, Fe_2O_3, Cr_2O_3 and Sb_2O_4, due to their chemical, magnetic, electrical and catalytic properties are particularly attractive for basic research and for a large number of prospective applications. Usually mixtures of oxides and compounds forming from them as well as the solid solutions of the structures of these compounds, show better properties from the viewpoint of applications than individual oxides [1–4]. Tetragonal MM^1SbO_6, where M = Cr, Fe, Rh; M^1 = Ge, Ru, Sn, Te, Ti, V of rutile-type structures have been reported and characterised recently because of their interesting functional properties [5–8]. It is known that iron–antimony–vanadium oxide catalysts are active and selective in several partial oxidation reactions, including the oxidative dehydrogenation of butenes [9,10], oxidative dehydrogenation of ethylbenzene [11,12], propylene oxidation [13,14], oxidation of methanol and alkylaromatics [15], propene and propane ammoxidation [16–18].

The properties of the components of the $FeVSbO_6$–$CrVSbO_6$ system are well known [7,8,19,20]. $FeVSbO_6$ and $CrVSbO_6$ are isostructural, crystallise in the tetragonal system and have rutile-type structures. The calculated unit cell parameters of $FeVSbO_6$ are the following: $a = b = 0.4604(4)$ nm, $c = 0.3053(3)$ nm, $V = 0.0647$ nm^3, $Z = 2$ [8]. Ternary Fe–V–Sb oxide is colour and melts incongruently at ~1280 °C with a deposition of solid Fe_2O_3 [8].

The calculated unit cell parameters of $CrVSbO_6$ are the following: $a = b = 0.45719(12)$ nm, $c = 0.30282(8)$ nm, $V = 0.0633$ nm^3, $Z = 2$ [7]. $CrSbVO_6$ is graphite-black and melts incongruently at ~1300 °C with a deposition of solid Cr_2O_3 [7].

It has been shown earlier that the compounds $FeVSbO_6$ and $CrVSbO_6$, are formed, upon heating of equimolar mixtures of V_2O_5 with α-Sb_2O_4 and Fe_2O_3 or Cr_2O_3 at temperatures up to 800 °C [7,8].

The compounds $FeVSbO_6$ and $CrVSbO_6$ have been investigated by SEM and IR methods [7,8] as well as by EPR in the range 277–573 °C [19,20]. A comparison of paramagnetic centres and interactions in $FeSbVO_6$ and $CrSbVO_6$ compounds has been made. The observed differences could be explained by different paramagnetic properties of Fe^{3+} and Cr^{3+} ions and differences in their interactions the V^{4+} ions [19].

As for the compounds, $FeVSbO_6$ and $CrVSbO_6$, because of isostructural character of the $MVSbO_6$ phases and similar values of Fe^{3+} and Cr^{3+} radii, the formation of continuous substitution solid solutions is expected. In view of the fact that the phase relations in the $FeVSbO_6$–$CrVSbO_6$ system have not been investigated yet, it has been deemed advisable to undertake works on the resolution of this problem.

2. Experimental

The polycrystalline samples for investigation were synthesised using traditional solid state methods by multistage heating of a mixture of initial components.

The following starting oxides were used in the experiments: Fe_2O_3, a.p. (POCh, Poland), Cr_2O_3, a.p. (POCh, Poland), V_2O_5, a.p. (POCh, Poland) and α-Sb_2O_4 which was obtained by oxidation of commercial Sb_2O_3 a.p. (Fluka, Germany) in air under conditions: 500 °C (24 h) → 550 °C (72 h).

The samples for the synthesis of new solid solutions were prepared from appropriate mixtures of oxides and from the specially synthesised compounds: $FeVSbO_6$ and $CrVSbO_6$ (Table 1). The compounds $FeVSbO_6$ and $CrVSbO_6$ have been prepared by the procedures given in works [7,8].

* Corresponding author.
E-mail address: elafil@zut.edu.pl (E. Filipek).

0925-8388/$ – see front matter © 2012 Elsevier B.V. All rights reserved.
doi:10.1016/j.jallcom.2012.01.092

Table 1
The composition of initial mixtures and the results of XRD analysis of the samples from the system $FeVSbO_6$–$CrVSbO_6$ after the last heating stage.

Composition of initial mixtures							Phases detected after last heating stage
No.	Contents of oxides [mol%]				Contents of compounds [mol%]		
	Fe_2O_3	Cr_2O_3	V_2O_5	Sb_2O_4	$FeVSbO_6$	$CrVSbO_6$	
1	31.67	1.67	33.33	33.33	95.00	5.00	$Fe_{0.95}Cr_{0.05}VSbO_6$
2	25.00	8.34	33.33	33.33	75.00	25.00	$Fe_{0.75}Cr_{0.25}VSbO_6$
3	16.67	16.67	33.33	33.33	50.00	50.00	$Fe_{0.50}Cr_{0.50}VSbO_6$
4	8.34	25.00	33.33	33.33	25.00	75.00	$Fe_{0.25}Cr_{0.75}VSbO_6$
5	3.34	30.00	33.33	33.33	10.00	90.00	$Fe_{0.10}Cr_{0.90}VSbO_6$

The mixtures of initial oxides or compounds after mechanical homogenisation by grinding in an agate mortar, shaped into pellets were heated in the atmosphere of air or an argon gas flow at temperatures from 620 to 800 °C with intermediate grinding of the reagents. The samples of reagents were heated at 620, 650, 700, 750 and 800 °C in 24 h stages.

On each heating stage the samples were gradually cooled to room temperature and their mass changes and their colour were recorded. After grinding and before shaping them again into pellets for the next heating stage, the samples were analysed by XRD and DTA/TG methods. When the diffraction patterns of samples taken after two consequent heating stages were identical both with respect to the positions (2θ) and to the intensities of the recorded diffraction lines (I/I_0), the procedure of heating samples was then finished. On the last heating stage the samples were investigated, apart from XRD measurement, by means of the DTA/TG and IR spectroscopy methods.

The powder diffraction patterns of obtained samples were recorded with the aid of the diffractometer HZG-4 (NRD) using the radiation CuK_α/Ni. Identification of phases was conducted on the basis of XRD characteristics contained in the PDF cards [21]. The powder diffraction patterns of $Fe_{1-x}Cr_xVSbO_6$ were indexed by means of POWDER program [22,23].

The densities of monophase samples were determined by degassing samples and hydrostatic weighing in pycnometric liquid (CCl_4) by the method described in paper [24].

The DTA/TG investigations all samples were performed by means of an F. Paulik–L. Paulik–L. Erdey derivatograph, product of MOM Budapest. The measurements were conducted in the air and argon in the temperature range 20–1000 °C, at the DTA galvanometer sensitivity of 1/5 and a constant heating rate of 10°/min. Some samples were subjected to DTA/TG using a TA Instruments SDT 2960. Measurements were conducted only in atmosphere of argon in the temperature range 20–1400 °C.

Initial mixtures and monophase samples were also examined by IR spectroscopy. The measurements were made within the wave number range of 1200–250 cm^{-1} (resolution 4 cm^{-1}) using a spectrophotometer IR SPECORD 80 (Carl Zeiss, Jena, Germany) applying a technique of pastilling under pressure. The sample were mixed with dehydrated KBr in a mass ratio of 1:300 and then pressed to pellets.

The chemical analysis of metallic elements' contents was performed for $Fe_{1-x}Cr_xVSbO_6$ ($0 \le x \le 1.0$) by means of scanning electron microscope (SEM) (JSM-1600, Jeol, Japan) with an X-ray energy dispersive analysis (EDX) (ISIS-300, Oxford).

3. Results and discussion

X-ray phase analysis (XRD), differential thermal analysis (DTA) and IR spectroscopy have shown that continuous substitution solid solutions of the formula $Fe_{1-x}Cr_xVSbO_6$ where $0 < x < 1$ are formed in the $FeVSbO_6$–$CrVSbO_6$ system according to the reactions:

$$(1-x)Fe_2O_{3(s)} + xCr_2O_{3(s)} + V_2O_{5(s)} + Sb_2O_{4(s)} = 2Fe_{1-x}Cr_xVSbO_{6(s.s.)} \quad (1)$$

$$(1-x)FeVSbO_{6(s)} + xCrVSbO_{6(s)} = Fe_{1-x}Cr_xVSbO_{6(s.s.)} \quad (2)$$

The diffraction patterns of preparations obtained both from the oxides and from previously prepared $FeVSbO_6$ and $CrVSbO_6$ showed, on the last heating stages, the presence of the set of diffraction lines that were shifted towards higher diffraction angles (2Θ) in comparison to the set of the lines characteristic of the $FeVSbO_6$ compound. In comparison to the diffraction pattern of $CrVSbO_6$, these lines were shifted towards smaller angles, so they corresponded to bigger d values. Fig. 1 shows fragments of diffraction patterns (XRD) recorded for the samples after the last stage of heating, whose composition corresponds to the formulas: $Fe_{0.95}Cr_{0.05}VSbO_6$, $Fe_{0.5}Cr_{0.5}VSbO_6$ and $Fe_{0.10}Cr_{0.90}VSbO_6$.

On the basis of the diffraction patterns, it can be concluded that in the $FeVSbO_6$–$CrVSbO_6$ system continuous solid solutions are formed and their general formula can be written as $Fe_{1-x}Cr_xVSbO_6$ (Fig. 2).

The analysis of the diffraction patterns of the obtained $Fe_{1-x}Cr_xVSbO_6$ solid solutions proved that with increasing x, the interplanar distances (d), characteristic of these solutions, decreased in comparison to pure $FeVSbO_6$ and approached to the values characteristic of $CrVSbO_6$.

Fig. 3 presents, apart from a fragment of a diffraction pattern of a mixture of 33.33 mol% V_2O_5, 33.33 mol% α-Sb_2O_4, 16.67 mol% Fe_2O_3 and 16.67 mol% Cr_2O_3 (curve a), fragments of the diffraction patterns of this sample after first heating stage, i.e. at 620 °C - 24 h (curves b) as well as a diffraction pattern of a monophase sample containing only $Fe_{0.5}Cr_{0.5}VSbO_6$ (curve c).

In the diffraction pattern of this sample after the first heating stage (Fig. 2b), apart from lines characteristic for the oxides, α-Sb_2O_4, V_2O_5, Cr_2O_3 and Fe_2O_3, a set of diffraction lines was present the position of which was near to that of lines characterising both

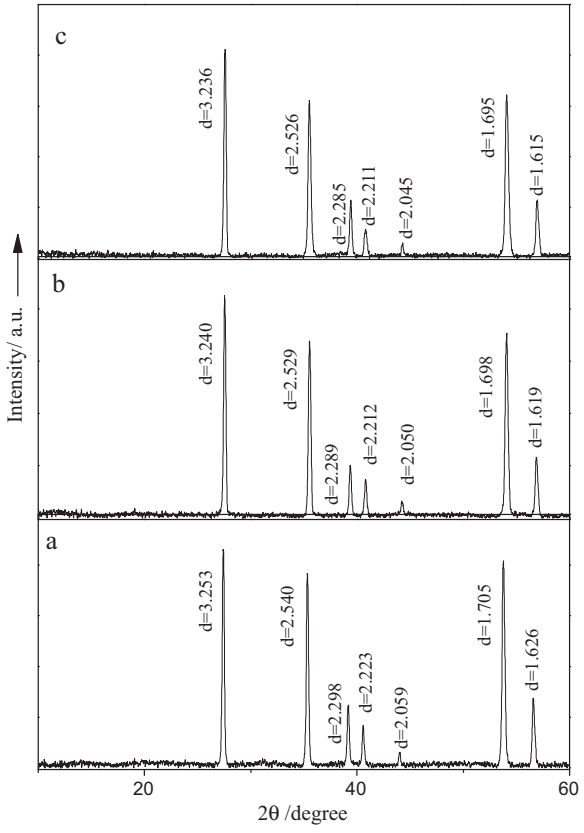

Fig. 1. XRD paterns of the selected solid solutions.

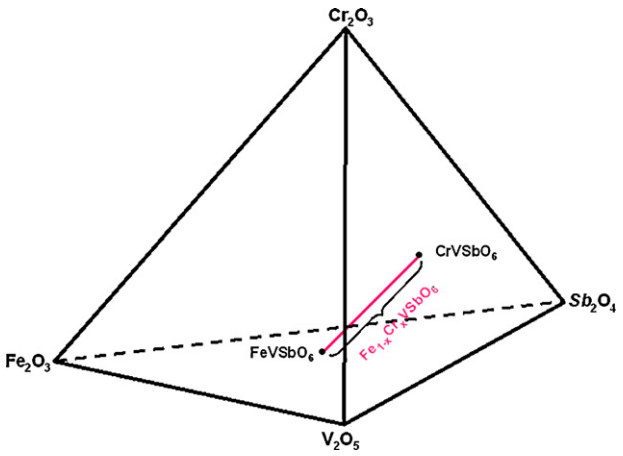

Fig. 2. Concentration tetrahedron of the Fe_2O_3–Cr_2O_3–V_2O_5–α-Sb_2O_4 system with position of new solid solutions $Fe_{1-x}Cr_xVSbO_6$.

$FeVSbO_6$ and $CrVSbO_6$, i.e. to $Fe_{1-x}Cr_xVSbO_6$. Phase analysis of this sample after the last heating stage at 800 °C showed that it contained only solid solution with formula $Fe_{0.5}Cr_{0.5}VSbO_6$ (Fig. 2c).

On the basis of the X-ray diffraction patterns of the $Fe_{1-x}Cr_xVSbO_6$ solid solutions for $x = 0.05$, 0.25, 0.50, 0.75 and 0.90 parameters and volumes of their unit cells were calculated by using program POWDER. Table 2 shows parameters and volumes of the unit cells of pure $FeVSbO_6$ [8] and $CrVSbO_6$ [7] phases as well as

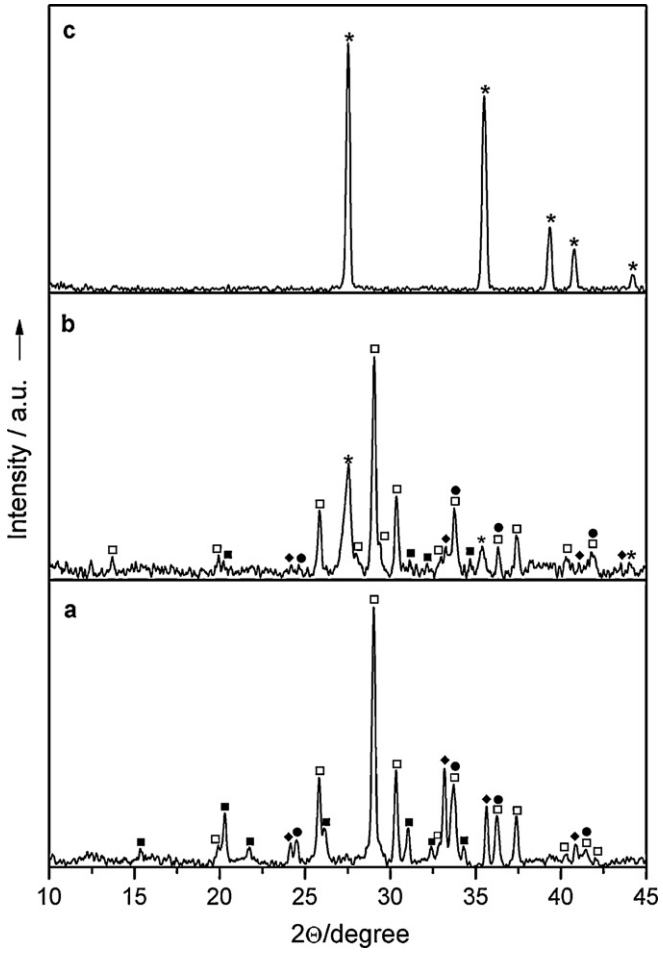

Fig. 3. The changes in powder diffraction patterns on selected stages of synthesis of the $Fe_{0.5}Cr_{0.5}VSbO_6$: (●) Cr_2O_3, (♦) Fe_2O_3, (■) V_2O_5, (□) α-Sb_2O_4, (*) $Fe_{0.5}Cr_{0.5}VSbO_6$.

Table 2
Unit cell parameters and volumes for the $FeVSbO_6$ ($x = 0$) and $CrVSbO_6$ ($x = 1.0$) phases and solid solutions $Fe_{1-x}Cr_xVSbO_6$.

x in $Fe_{1-x}Cr_xVSbO_6$	a [nm]	b [nm]	c [nm]	V [nm^3]
0.00	0.46040	0.46040	0.30530	0.06470
0.05	0.45998	0.45998	0.30506	0.06455
0.25	0.45947	0.45947	0.30465	0.06432
0.50	0.45876	0.45876	0.30426	0.06403
0.75	0.45801	0.45801	0.30324	0.06361
0.90	0.45748	0.45748	0.30301	0.06342
1.00	0.45719	0.45719	0.30282	0.06330

those of solid solutions for $x = 0.05$, 0.25, 0.50, 0.75 and 0.90. The data in Table 2 point to the fact that with the increasing degree of incorporation of Cr^{3+} ions in the place of Fe^{3+} ions the contraction of the crystal lattice and consequential decrease in the unit cell volumes take place (Fig. 4).

All monophase samples, i.e. comprising only $Fe_{1-x}Cr_xVSbO_6$ where $x = 0.05$, 0.25, 0.50, 0.75 and 0.90, were examined by DTA/TG, both in air and argon, up to 1000 °C. The DTA curves of $Fe_{1-x}Cr_xVSbO_6$ obtained from V_2O_5, Fe_2O_3 and Cr_2O_3 with α-Sb_2O_4 as well as from mixtures $FeVSbO_6$ with $CrVSbO_6$ show no thermal effects up to 1000 °C. Furthermore, the TG curves of these samples do not indicate any mass losses. The DTA/TG data indicate that this phase is stable up to at least 1000 °C.

The next stage of the research was, aimed at establishing the thermal stability of selected monophase samples containing $Fe_{1-x}Cr_xVSbO_6$ where $x = 0.25$, 0.50 and 0.75, in temperatures up to 1400 °C only in argon atmosphere. The tests were not conducted in air atmosphere for technical reasons. The manufacturer recommended against conducting DTA/TG in air at the temperatures above 1000 °C.

Differential thermal analysis of selected monophase samples containing $Fe_{1-x}Cr_xVSbO_6$ where $x = 0.25$, 0.50, 0.75, conducted up to 1400 °C in argon atmosphere, revealed the presence of one endothermic effect at ~1350 °C, as shown in Fig. 5. With increasing x the onset temperature of this effect did not change significantly. According to literature data the temperature of this effect is close to that of thermal decomposition of $CrSbO_4$ [25].

On the other hand, the TG curves (Fig. 5) of the samples investigated up to 1400 °C revealed their mass decrement starting at ~1050 °C, fluctuating between 45.15 and 66.13% by weight.In view of the hitherto performed studies, it can be claimed that the mass decrement is due to a thermal decomposition of the solid solution, i.e. $Fe_{1-x}Cr_xVSbO_6$, accompanied by liberation of $Sb_4O_{6(g)}$. For the sample containing $Fe_{0.5}Cr_{0.5}VSbO_6$ the mass loss up to 1350 °C was

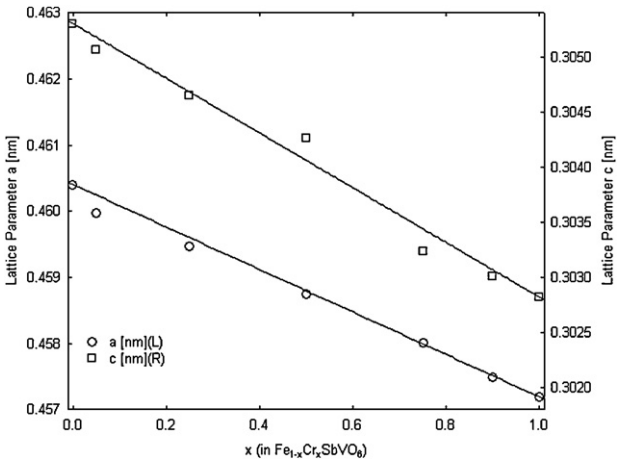

Fig. 4. Lattice parameter of $Fe_{1-x}Cr_xVSbO_6$ solid solution.

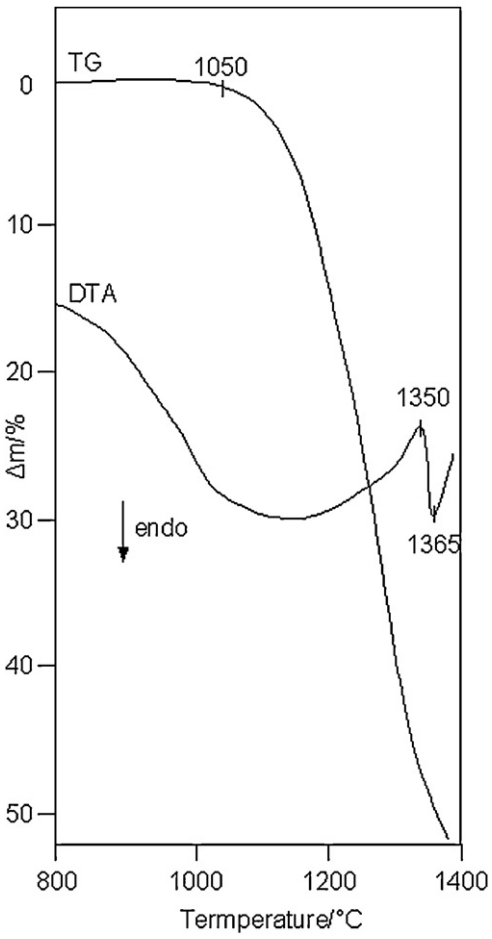

Fig. 5. DTA-TG curves of $Fe_{0.5}Cr_{0.5}VSbO_6$.

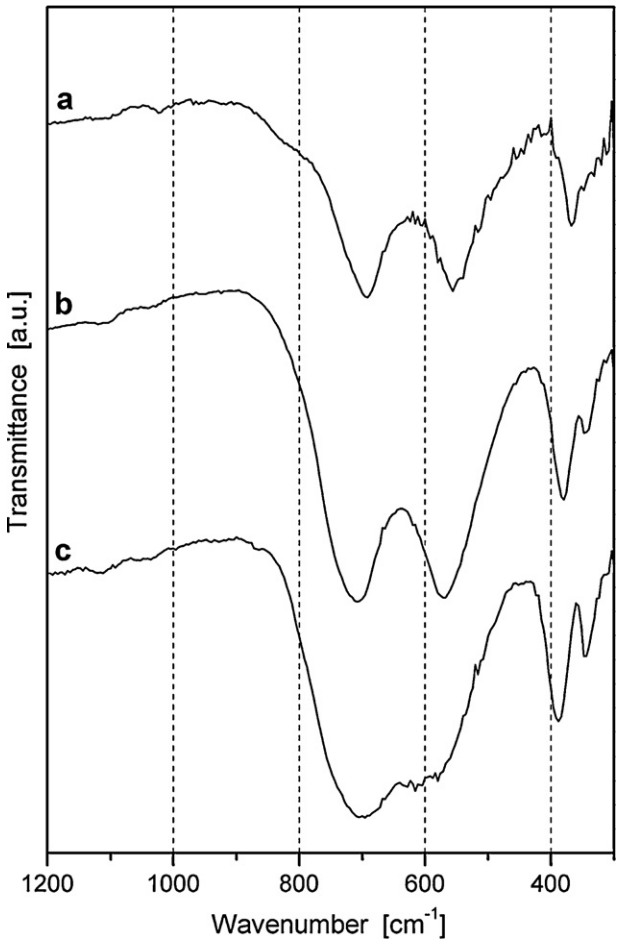

Fig. 6. IR spectra of (a) $FeVSbO_6$; (b) $Fe_{0.5}Cr_{0.5}VSbO_6$ and (c) $CrVSbO_6$.

48.88%, which is in good agreement with that calculated from the equation:

$$4Fe_{0.5}Cr_{0.5}VSbO_{6(s.s.)} \rightarrow 2CrSbO_{4(s)} + Fe_2O_{3(s)} + 2V_2O_{5(l)} + \tfrac{1}{2}Sb_4O_{6(g)} \quad (3)$$

XRD analysis of the samples containing the solid solution $Fe_{1-x}Cr_xVSbO_6$ ($0.25 \le x \le 0.75$), additionally heated at 1300 °C (1 h), that is a temperature close to the onset of the endothermic effect recorded on the DTA curves, and then rapidly cooled, confirmed the course of their decomposition. The phase analysis of the obtained preparations showed that apart from the phases having crystallised from the liquid, e.g. V_2O_5 they contained also a phase identified as $CrSbO_4$ and the oxide Fe_2O_3.

Solid solutions with different compositions, were examined by IR spectroscopy. Fig. 6 shows IR spectra of the $FeVSbO_6$ phase (curve a), of the $Fe_{0.5}Cr_{0.5}VSbO_6$ solid solution (curve b) and of the $CrVSbO_6$ phase (curve c).

The spectra are distinguished by a very similar distribution of their absorption bands. IR spectrum of the $Fe_{0.5}Cr_{0.5}VSbO_6$ solid solution (Fig. 6, curve b) contains absorption bands with their maxima lying at 705, 570, 375 and 340 cm^{-1}, respectively. It follows from the literature survey that these bands are characteristic and were observed in the IR spectra of solid vanadates (V) and antimonates (V) with the rutile type structure [25–27]. Intensive band with an absorption maximum at 705 cm^{-1} can probably be attributed to the M—O—M bridge bonds stretching [28]. The next band which shows distinct maximum at 570 cm^{-1} in the light of accessible literature can be ascribed to the stretching bonds of Sb—O in SbO_6 [29,30], Fe—O in FeO_6 octahedra [31–33] as well as to stretching vibrations of the bonds Cr—O in CrO_6 octahedra [34,35]. The position of the other bands in a vibration spectrum of $Fe_{0.5}Cr_{0.5}VSbO_6$, i.e. of those at 375 cm^{-1} and 340 cm^{-1}, implies that they were developed by deformation vibrations of the O—M—O (O—Fe—O, O—Sb—O, O—V—O) and V—O bonds in the distorted MO_6 octahedra or they are mixed character [8,21,23,27,36–39].

The IR spectrum of $Fe_{0.5}Cr_{0.5}VSbO_6$, a phase whose structure has not previously been known, implies that it is built from MO_6 (where M = V, Fe, Cr, Sb) octahedra and adopts a rutile type structure.

A series of IR spectra characteristic of solid solutions of $Fe_{1-x}Cr_xVSbO_6$ type with different compositions (x) have shown that with increasing degree of the Cr^{3+} ion incorporation into the $FeVSbO_6$ lattice, the absorption bands are shifted towards higher wave numbers.

Then the morphologies of the polycrystalline $FeVSbO_6$, $CrVSbO_6$ and $Fe_{1-x}Cr_xVSbO_6$ were studied by scanning electron microscopy (SEM) with an X-ray energy dispersive analysis (EDX) probe to determine the (V + Sb):(Fe + Cr) ratio in various parts of the samples.

Usually from 3 to 5 determinations for morphologically equivalent areas were made and the mean error in determination of the (V + Sb):(Fe + Cr) ratio may be estimated as about 5%.

Fig. 7 presents a SEM image of the $FeVSbO_6$ (a), $CrVSbO_6$ (b) and a SEM image of the new solid solution – $Fe_{0.5}Cr_{0.5}VSbO_6$ (c).

The crystals visible in Fig. 7a and b are similar by their morphology to the crystals of $Fe_{0.5}Cr_{0.5}VSbO_6$ (Fig. 7c.) but differ in size. The SEM images of $FeVSbO_6$ and $CrVSbO_6$ reveal irregular crystals of sizes from ~0.75 to 4 μm. SEM image of $Fe_{0.5}Cr_{0.5}VSbO_6$ (Fig. 7c) showed the presence of only one of crystals' habit. Crystals of $Fe_{0.5}Cr_{0.5}VSbO_6$ are irregular in shape and the average their size is about 0.5 μm. The sizes of the largest crystals are of the order

Table 3
Metal composition of selected monophase samples as determined by SEM/EDX analysis.

Formula $Fe_{1-x}Cr_xVSbO_6$	Experimental composition [at.%]				Composition calculated from formula [at.%]				$\frac{V+Sb}{Cr+Fe}$ (exp/cal)
	Fe	Cr	Sb	V	Fe	Cr	Sb	V	
$FeVSbO_6$ ($x = 0.00$)	32.85	–	33.71	33.44	33.33	–	33.33	33.34	2.044/2.000
$Fe_{0.75}Cr_{0.25}VSbO_6$ ($x = 0.25$)	23.97	9.06	31.94	35.03	25.00	8.33	33.33	33.34	2.028/2.000
$Fe_{0.50}Cr_{0.50}VSbO_6$ ($x = 0.50$)	16.05	16.60	34.34	33.02	16.67	16.66	33.33	33.34	2.032/2.000
$Fe_{0.25}Cr_{0.75}VSbO_6$ ($x = 0.75$)	7.99	24.80	34.57	32.64	8.33	25.00	33.33	33.34	2.050/2.000
$CrVSbO_6$ ($x = 1.00$)	–	33.36	34.45	32.19	–	33.33	33.33	33.34	1.998/2.000

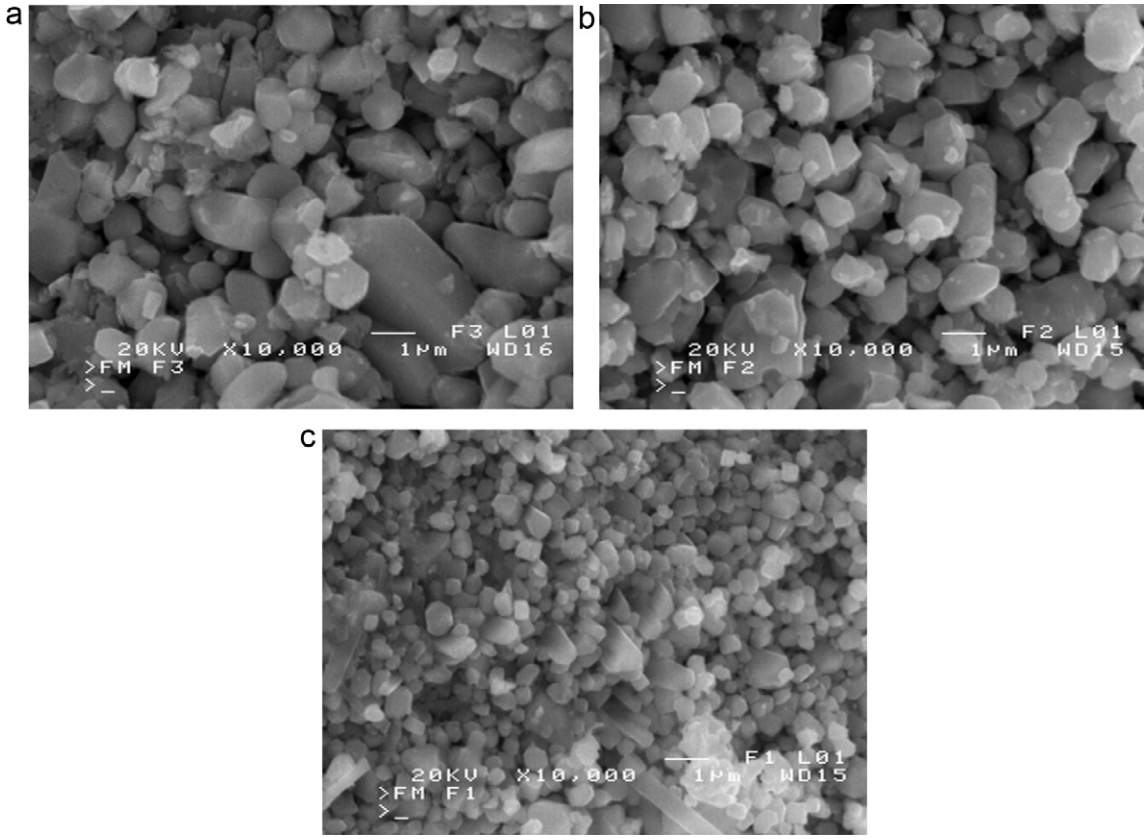

Fig. 7. SEM images of the $FeVSbO_6$ (a), $CrVSbO_6$ (b) and $Fe_{0.5}Cr_{0.5}VSbO_6$ (c).

of 2.5 μm whereas the size of smaller crystals do not often exceed 0.35 μm.

The results of experimental determination of composition by EDX analysis of monophase samples (Table 3) showed that the (V + Sb):(Fe + Cr) ratios corresponded to the calculated values from formula of the new solid solutions, i.e. $Fe_{1-x}Cr_xVSbO_6$.

Very similar experimental and calculated contents of Cr, Fe, V and Sb in analysed phases confirm the validity of the proposed formula for new solid solution $Fe_{1-x}Cr_xVSbO_6$.

4. Conclusions

(1) Some continuous substitution solid solutions of $Fe_{1-x}Cr_xVSbO_6$ type are formed in the $FeVSbO_6$–$CrVSbO_6$ system.
(2) With increasing x in $Fe_{1-x}Cr_xVSbO_6$ the crystal lattices of the solid solutions formed undergo increasing contraction, measured in terms of decreasing volumes of unit cells and a shift in the position of IR absorption bands towards higher wave numbers.
(3) The new phase is built of MO_6 (where M = V, Fe, Cr, Sb) octahedra and adopts a rutile-type structure.
(4) Solid solution $Fe_{1-x}Cr_xVSbO_6$ decomposes in the solid state in argon at ~1050 °C. The solid products of decomposition of the investigated solution are $CrSbO_4$ and Fe_2O_3.

References

[1] P.M. Kulal, D.P. Dubal, C.D. Lokhande, V.J. Fulari, J. Alloys Compd. 509 (2011) 2567–2571.
[2] G.A. El-Shobaky, A.I. Ahmed, H.M.A. Hassan, S.E. El-Shafey, J. Alloys Compd. 509 (2011) 1314–1321.
[3] G. Wu, X. Tan, G. Li, C. Hu, J. Alloys Compd. 504 (2010) 371–376.
[4] J. Nilsson, A. Landa-Canovas, S. Hansen, A. Andersson, Catal. Today 33 (1997) 97–108.
[5] J. Isasi, M.L. Veiga, C. Pico, J. Mater. Sci. Lett. 15 (1996) 1022–1024.
[6] J. Isasi, M.L. Veiga, C. Pico, J. Mater. Chem. 5 (1995) 871–874.
[7] E. Filipek, G. Dąbrowska, J. Mater. Sci. 42 (2007) 4905–4916.
[8] E. Filipek, G. Dąbrowska, M. Piz, J. Alloys Compd. 490 (2010) 93–97.
[9] R. Häggblad, M. Massa, A. Andersson, J. Catal. 266 (2009) 218–227.
[10] Ch. Zhang, C.R.A. Catlow, J. Phys. Chem. C 112 (2008) 9783–9797.
[11] M.S. Park, V.P. Vislovskiy, J.S. Chang, Y.G. Shul, J.S. Yoo, S.E. Park, Catal. Today 87 (2003) 205–212.
[12] A. Sun, Z. Qin, S. Chen, J. Wang, J. Mol. Catal. A 210 (2004) 189–195.
[13] Ch.T. Wang, D.L. Lai, J. Am. Ceram. Soc. 94 (8) (2011) 2646–2651.
[14] R.G. Teller, J.F. Brazdil, R.K. Grasselli, J. Chem. Soc. Faraday Trans. 81 (1985) 1693–1704.
[15] H. Golinska-Mazwa, P. Decyk, M. Ziolek, J. Catal. 284 (1) (2011) 109–123.

[16] M.O. Guerrero-Pérez, J.L.G. Fierro, M. Vicente, M.A. Bañares, Chem. Mater. 19 (2007) 6621–6628.
[17] H. Roussel, B. Mehlomakulu, F. Belhadj, E. van Steen, J.M.M. Millet, J. Catal. 205 (2002) 97–106.
[18] N. Ballarini, F.J. Berry, F. Cavani, M. Cimini, X. Ren, D. Tamoni, F. Trifiro, Catal. Today 128 (2007) 161–167.
[19] J. Typek, N. Guskos, E. Filipek, M. Piz, Rev. Adv. Mater. Sci. 23 (2010) 196–206.
[20] J. Typek, N. Guskos, E. Filipek, J. Non-Cryst. Solids 354 (2008) 4494–4499.
[21] Powder Diffraction File, International Center for Diffraction Data, Swartmore (USA), 1989.
[22] D. Taupin, Appl. Crystallogr. 1 (1968) 178–181.
[23] D. Taupin, J. Appl. Crystallogr. 6 (1973) 380–385.
[24] Z. Kluz, I. Waclawska, Roczniki Chem. 49 (1974) 839–841.
[25] E. Filipek, M. Kurzawa, G. Dąbrowska, J. Therm. Anal. Cal. 60 (2000) 167–171.
[26] J. Walczak, E. Filipek, M. Bosacka, Solid State Ionics 101–103 (1997) 1363–1367.
[27] N. Ballarini, F. Cavani, C. Giunchi, S. Masetti, F. Trifiro, D. Ghisletti, U. Cornaro, R. Catani, Top. Catal. 15 (2001) 111–119.
[28] E. Filipek, The Synthesis and Physicochemical Properties of New Phases in the Systems Oxides V_2O_5, MoO_3, α-Sb_2O_4 (Polish), Editorial office - Szczecin University of Technology, 2007, ISBN 978-83-7457-025-1 (in Polish).
[29] R. Franck, C. Rocchiccioli-Deltcheft, J. Guillerment, Spectrochim. Acta 30A (1974) 1–14.
[30] F. Sala, F. Trifiro, J. Catal. 41 (1976) 1–13.
[31] V. Kozhukharov, S. Nikolov, M. Marinov, T. Troev, Mater. Res. Bull. 14 (1979) 735–741.
[32] J. Preudhomme, P. Tarte, Spectrochim. Acta 27A (1971) 1817–1835.
[33] R. Iordanova, Y. Dimitriev, V. Dimitriov, D. Klissurski, J. Non-Cryst. Solids 167 (1994) 74–80.
[34] A. Bielański, J. Poźniczek, E. Wenda, Bull. Acad. Pol. Sci. Ser. Sci. Chim. 6 (1976) 485–492.
[35] M.A. Nabar, D.S. Phanasgaonkar, Spectrochim. Acta 39 (1983) 777–779.
[36] E. Husson, Y. Repelin, H. Brusset, A. Cerez, Spectrochim. Acta 35A (1979) 1177–1187.
[37] J. Hanuza, K. Hermanowicz, W. Ogonowski, B. Jeżowska-Trzebiatowska, Bull. Acad. Pol. Sci. Ser. Sci. Chim. 31 (1983) 139–152.
[38] J. Muller, J.C. Joubert, J. Solid State Chem. 14 (1975) 8–13.
[39] S. Bahfenne, R.L. Frost, Appl. Spectrosc. Rev. 45 (2010) 101–129.